Coexistence of Parametric Decay Cascades and Caviton Collapse at Subcritical Densities

D. F. DuBois,[(1)] Harvey A. Rose,[(1)] and David Russell[(2)]
[(1)]*Los Alamos National Laboratory, MS B262, Los Alamos, New Mexico 87545*
[(2)]*Lodestar Research Corporation, 2400 Central Avenue, Boulder, Colorado 80301*
(Received 26 December 1990)

We report results of two-dimensional numerical solutions of Zakharov's model for strong Langmuir turbulence excited by powerful electromagnetic pump waves at subcritical densities, as in hf modification of the ionosphere and laser-plasma interactions. The results show that truncated parametric decay cascades can coexist with caviton collapse for moderate pump power. A high level of ion density fluctuations, driven primarily by caviton collapse, produces energy and power spectra which are not consistent with conventional weak turbulence theory.

PACS numbers: 52.35.Ra, 52.35.Mw, 94.20.−y

In the last few years it has become evident[1,2] that the short-time-scale properties of the plasma turbulence induced in the ionospheric F layer by hf "heating" can be successfully described by the so-called strong Langmuir turbulence[3,4] (SLT) theory. In this theory a significant fraction of the high-frequency electrostatic energy is contained in nonlinear objects called cavitons which undergo cycles of nucleation, collapse, and burnout.

SLT theory describes the plasma line fluctuation power spectrum measured by Thomson scattering radars at Arecibo in the first tens of ms following the onset of the heating pulse in low duty cycle heating[1,5] and in cw heating from a "cold start."[6,7] The power spectrum (for the up-shifted plasma line) consists of a broad, relatively featureless, *caviton continuum* lying mostly below the heater frequency ω_H and *a free mode peak* lying above the heater frequency at the location of the Langmuir frequency.

The conventional weak turbulence theory (WTT) fails to explain *any* aspect of this spectrum. The sharpness of the free-mode line and its frequency location indicates that it arises from turbulence in a narrow (<100 m) layer near the reflection density. This is consistent with the recent observations of Djuth, Sulzer, and Elder.[6]

At times of the order of 30–100 ms following turn-on, Djuth, Sulzer, and Elder[6] and Fejer, Sulzer, and Djuth[7] find that the turbulence spreads to unevenly fill a layer 1–2 km below the reflection height. On this same time scale[1,5,7,8] the plasma line power spectrum intensifies and develops sharp spectral features at frequencies below ω_H. The location of these features down-shifted at approximately units of 1:3:5: $\cdots$ times the ion acoustic frequency kc_s can be identified with a cascade of parametric decay interactions.

For the parametric decay of the heater wave we have the matching condition

$$\omega_H = [\omega_p^2(z_1) + 3\tilde{k}_1^2 v_e^2 + \omega_c^2 \sin^2\theta]^{1/2} + |\tilde{k}_1| c_s$$

which determines $\omega_p(z_1)$ the electron plasma frequency at the "matching" altitude z_1 if $\tilde{\mathbf{k}}_1$ is taken to be $\tilde{\mathbf{k}}$ observed by the radar; here v_e^e is the electron thermal velocity, ω_c is the electron gyrofrequency, and θ is the angle between $\mathbf{k}_1$ and the geomagnetic field $\mathbf{B}_0$. The simulation studies reported here are based on two-dimensional simulations of Zakharov's equation for the Langmuir envelope electric field $\mathbf{E}(\mathbf{x},t)$ and the fluctuation of the ion density from its mean value $n(\mathbf{x},t)$. The equations and simulation procedures are the same as discussed in detail in I.[4] The major difference is in the value of the heater frequency parameter defined in I: $\tilde{\omega}_0 = \omega_H - \omega_p(z)$. We again consider the case of a spatially uniform heater wave in the envelope approximation used in I: $\tilde{\mathbf{E}}_0(t) = \tilde{\mathbf{E}}_0 \exp(-i\tilde{\omega}_0 t)$, where $\tilde{\mathbf{E}}_0$ and $\mathbf{B}_0$ both lie along the x direction. Whereas in I we mainly treated cases where $\tilde{\omega}_0 < \frac{3}{2}(\tilde{k}\lambda_D)^2\omega_p$ (i.e., $\omega_0 < k^2$ in the scaled units of I), appropriate to near critical density, here we consider the complementary case, $\omega_0 > k^2$.

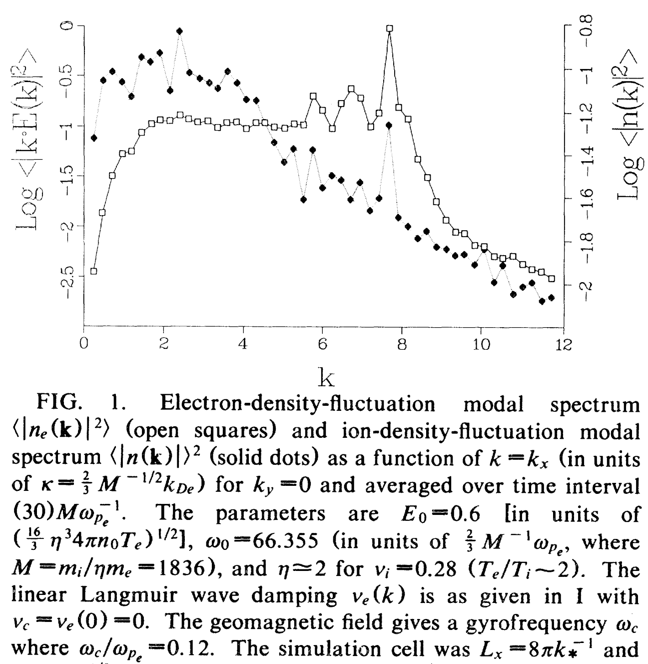

FIG. 1. Electron-density-fluctuation modal spectrum $\langle |n_e(\mathbf{k})|^2 \rangle$ (open squares) and ion-density-fluctuation modal spectrum $\langle |n(\mathbf{k})| \rangle^2$ (solid dots) as a function of $k = k_x$ (in units of $\kappa = \frac{2}{3} M^{-1/2} k_{De}$) for $k_y = 0$ and averaged over time interval $(30) M \omega_{p_e}^{-1}$. The parameters are $E_0 = 0.6$ [in units of $(\frac{16}{3}\eta^3 4\pi n_0 T_e)^{1/2}$], $\omega_0 = 66.355$ (in units of $\frac{2}{3} M^{-1} \omega_{p_e}$, where $M = m_i/\eta m_e = 1836$), and $\eta \simeq 2$ for $\nu_i = 0.28$ ($T_e/T_i \sim 2$). The linear Langmuir wave damping $\nu_e(k)$ is as given in I with $\nu_c = \nu_e(0) = 0$. The geomagnetic field gives a gyrofrequency ω_c where $\omega_c/\omega_{p_e} = 0.12$. The simulation cell was $L_x = 8\pi k_*^{-1}$ and $L_y = 3^{-1/2} 4\pi k_*^{-1}$, where $k_* = \kappa(1 - \nu_i^2)^{1/2}$ or 0.96 in scaled unit, and 512 (128) Fourier modes were used in the x (y) direction which results in marginal $\mathbf{k}$-space resolution. Unlike the case for the power spectra in Fig. 2, we expect these time-averaged modal spectra to be a fair representation of the ensemble-averaged spectra.

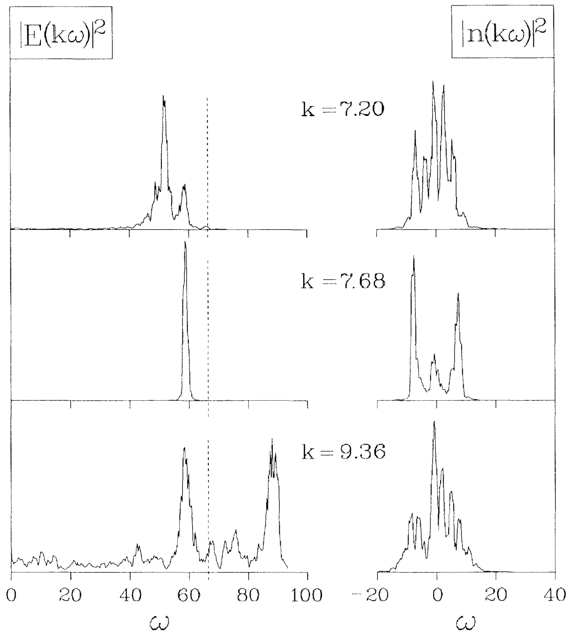

FIG. 2. Power spectra for $\langle|E(\mathbf{k},\omega)|^2\rangle$ and $\langle|n(\mathbf{k},\omega)|^2\rangle$, in arbitrary units, for three values of k_x and $k_y=0$. $k_x=7.68$ is the primary decay mode. $k_x=7.20$ and 9.36 are not in the primary cascade. The dashed line is ω_0. The parameters are the same as for Fig. 1.

In Fig. 1 we show time-averaged electron-density-fluctuation spectra in the well-developed, quasistationary turbulent state $k^2\langle|\mathbf{E}(\mathbf{k})|^2\rangle$ as a function of k_x for $k_y=0$ $(\theta=0)$ for typical simulation parameters. We note that, in addition to the primary cascade peaks at $k_1=7.68$, $k_3=k_1-k_*=6.72$, and $k_5=k_1-2k_*=5.76$, there is a broad background of turbulence which contains a significant fraction of the turbulent electrostatic energy and which is not accounted for in WTT. We also show, for the same parameters, the time-averaged ion fluctuation energy spectrum $\langle|n(k)|^2\rangle$. This spectrum, which is somewhat noisy due to the relatively short-time-averaging interval, is dominated by a broad spectrum associated with collapse and also contains a sharp feature at $k_1=7.68$ associated with the primary decay of the heater. We observe distinct decay lines for θ as large as 60°. The cascade structure becomes more diffuse as θ increases. We find that increasing E_0, above some value, with ω_0 fixed *decreases* the number of steps in the primary cascade, while increasing ω_0 with E_0 fixed *increases* the number of steps.

In Fig. 2 we show the power spectra $|\mathbf{E}(\mathbf{k},\omega)|^2$ for $k_y=0$ for several values of k_x. The power spectra

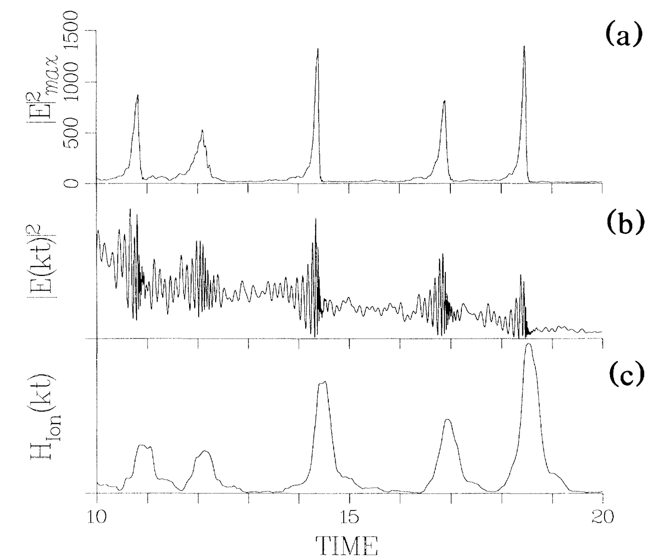

FIG. 3. Time series in the decaying turbulence resulting from turning off the pump (at time $=10$) in the stationary turbulence of Fig. 1: (from top to bottom) The maximum value of $|E|^2$ in the simulation cell, $|\mathbf{E}(\mathbf{k},t)|^2$ for $k_x=7.20$, $k_y=0$, and total ion-density-fluctuation energy in mode $\mathbf{k}$, $H_{\text{ion}}(\mathbf{k},t)=\frac{1}{2}|n(\mathbf{k},t)|^2+\frac{1}{2}k^{-2}|\partial_t n(\mathbf{k},t)|^2$. Time in units of $\frac{3}{2}M\omega_{p_e}^{-1}$. For the parameters of Fig. 1.

consist of free-mode peaks at $\omega\simeq k_x^2$ [i.e., $\tilde{\omega}-\omega_p \simeq \frac{3}{2}(\tilde{k}_x\lambda_D)^2\omega_p$ in physical units], embedded in a weaker broad continuum. As $\tilde{\omega}_0\rightarrow 0$ this continuum becomes the caviton continuum observed near critical density.[1,2] In Fig. 2 we also show ion fluctuation (ion line) power spectra for the same parameters.

In Fig. 3(a) is shown a time series during the decaying turbulence which persists after pump turnoff, in which caviton collapse events—the sharp peaks in the maximum of $|E(x,t)|^2$ in the simulation cell—are better separated in time than in the driven regime. In Fig. 3(c) is shown the time series of the total ion fluctuation energy in mode $\mathbf{k}$, $H_{\text{ion}}(\mathbf{k},t)$. Note the positive correlation of the peaks in $H_{\text{ion}}(\mathbf{k},t)$ with the collapse events in Fig. 3(a) which is consistent with collapse as the primary source of ion fluctuations. Dissipation rate diagnostics show that most of the electrostatic energy is dissipated by caviton collapse.

We can write the total electrostatic envelope field as $\mathbf{E}(\mathbf{x},t)=\mathbf{E}_c(\mathbf{x}t)+\mathbf{E}_f(\mathbf{x}t)$, where $\mathbf{E}_f(\mathbf{x},t)$ is the nonlocalized or free-Langmuir-wave (FLW) part. The localized or caviton part $\mathbf{E}_c$ can be written as a sum over $N(T)$ discrete events occurring during the observation time T (see I): $\mathbf{E}_c(\mathbf{x},t)=\sum_i \boldsymbol{\varepsilon}_i(\mathbf{x}-\mathbf{x}_i,t-t_i)$. With this decomposition we can write for the Fourier modes

$$|E(\mathbf{k},t)|^2=|E_f(\mathbf{k},t)|^2+|E_c(\mathbf{k},t)|^2+\sum_i 2|\varepsilon_i(\mathbf{k},t)||E_f(\mathbf{k},t)|\cos[\omega_k t-\mathbf{k}\cdot\mathbf{x}_i-\phi_i(t)]\,, \quad (1)$$

where we have written $E_f(\mathbf{k},t)=|E_f(\mathbf{k},t)|\exp(-i\omega_k t)$, and, from the observed power spectra, ω_k is close to the Bohm-Gross frequency. The caviton phase $\phi_i(t)$, obtained from $\varepsilon_i(kt)=|\varepsilon_i(k,t)|\exp[i\phi_i(t)]$, is a rapidly varying phase arising from the nucleation and collapse of cavitons.[4] The "buzzes" or fast modulations in $|\mathbf{E}(\mathbf{k},t)|^2$ in Fig. 3(b) can be identified with the rapidly varying interference terms in (4). From such considerations we estimate that in the case of the parameters of Figs. 1–3 that at low k ($k^2 \ll \omega_0$) about half of the total time-averaged energy is in free modes, while for $k^2 > \omega_0$ the fraction of free-mode energy decreases from about 50% to zero as k increases.

From studies of renormalized turbulence theories[9] we can abstract a heuristic, steady-state equation for the ensemble average of the free-Langmuir-wave power spectrum

$$\langle |E_f(\mathbf{k},\omega)|^2\rangle = S_L\{W_f;\mathbf{k},\omega\}[(\omega-\omega_k)^2+\gamma_L^2(\mathbf{k})]^{-1}, \quad (2)$$

where $W_f(\mathbf{k}) = (2\pi)^{-1}\int d\omega \langle |E_f(\mathbf{k},\omega)|^2\rangle$. The total free-mode (linear plus nonlinear) damping can be written (for $B_0 = 0$)

$$\gamma_L(\mathbf{k}) = \nu_e(\mathbf{k}) + |\hat{\mathbf{k}}\cdot \mathbf{E}_0|^2 R_n(\mathbf{k},k^2-\omega_0) + \int d\mathbf{k}'(\hat{\mathbf{k}}\cdot\hat{\mathbf{k}}')^2 W_f(\mathbf{k}')R_n(\mathbf{k}-\mathbf{k}',k^2-k'^2)$$
$$+\tfrac{1}{4}\int d\mathbf{k}'(\hat{\mathbf{k}}\cdot\hat{\mathbf{k}}')^2\langle |n(\mathbf{k}-\mathbf{k}',k^2-k'^2)|^2\rangle + \nu_{\text{cav}}(\mathbf{k}), \quad (3)$$

where

$$R_n(\mathbf{Q},\Omega) = 2\nu_i|\mathbf{Q}|^3\Omega\{[\Omega^2-|\mathbf{Q}|^2]^2+4\Omega^2|\mathbf{Q}|^2\nu_i^2\}^{-1},$$

$d\mathbf{k}' = d^Dk'(2\pi)^{-D}$ in D spatial dimensions, and[4] $\nu_i = \text{Im}\,\omega_i/\text{Re}\,\omega_i$, the ion acoustic damping ratio. The nonlinear source term is

$$S_L\{W_f;\mathbf{k},\omega\} = |\hat{\mathbf{k}}\cdot\mathbf{E}_0|^2\langle |n(\mathbf{k},\omega-\omega_0)|^2\rangle + \int d\mathbf{k}'(\hat{\mathbf{k}}\cdot\hat{\mathbf{k}}')^2\langle |n(\mathbf{k}-\mathbf{k}',\omega-k'^2)|^2\rangle W_f(\mathbf{k}') + S_{\text{cav}}(\mathbf{k}). \quad (4)$$

Qualitatively we can take the density-fluctuation spectrum $\langle |n(\mathbf{k},\omega)|^2\rangle$ to be that *observed* in the simulations. In these equations k is expressed in units of k_* and in the conventional scaled units the Langmuir wave frequency is $\omega_k = k^2$, the ion wave frequency is $\omega_s(k) = |\mathbf{k}|$, and the decay matching conditions can be written $k^2 = k'^2 \pm |\mathbf{k}-\mathbf{k}'|$. In this paper we will use this theory, which will be discussed in more detail elsewhere, to motivate a qualitative interpretation of the simulation results.

The first term in (3) is the linear (collisional plus Landau) damping, the second term the parametric gain (Stokes) or loss (anti-Stokes) induced by the pump, and the third term contains the gain and loss induced by Langmuir fluctuations. The last two terms are neglected in conventional treatments. The penultimate term is the scattering-out rate due to *ion fluctuation-induced* scattering of FLW's from collapse-enhanced ion fluctuations and the last term arises from the coupling of FLW's to cavitons.

In the conventional WTT treatment of the cascade, the source terms are neglected altogether and a singular spectrum results from the balancing of the linear damping against the second and third terms in (3). This leads to the well-known cascade solutions.[10–12] The number of steps in the cascade is roughly $m = |E_0|^2/|E_{0t}|^2$, where $|E_{0t}|^2 \simeq 2\nu_e(k_1)\nu_i$ is the threshold field for the parametric decay instability.[13] In our simulations $m \gg k_1/k_*$ so conventional WTT would predict an unlimited cascade to $k = 0$. We use this theory to define an effective Langmuir wave damping $\nu_{\text{eff}}(k)$ which is the sum of ν_e and the last two terms in (3). The second term in (3) destabilizes (stabilizes) the Stokes, $k = k_1$ (anti-Stokes, $k = k_1 + k_* = k_a$), modes, for which the third term is relatively weak, so that their damping decrements $\gamma_L(k_1)$ and $\gamma_L(k_a)$ are roughly $\nu_{\text{eff}} \mp |E_0|^2(2\nu_i)^{-1}$, respectively. Since the ratio of the powers in these modes in Fig. 1 is large, and their source terms are comparable we deduce that $\nu_{\text{eff}}(k_1) \sim |E_0|(2\nu_i)^{-1} \sim 1 \gg \nu_e(k_1)$ and $\nu_{\text{eff}}(k_1) \gg \gamma_L(k_1) \gg \nu_e(k_1)$. For stronger driving ($E_0 \sim 1.2$) (spectra not shown) the lines are dramatically broadened and the cascade modes are not stronger than their neighbors, implying $\nu_{\text{eff}}(k_1) \gg 1$. The ratio of $\nu_{\text{cav}}(k)/\nu_{\text{eff}}(k)$ still remains to be determined. Since $\nu_{\text{eff}} \gg \nu_e$, the number of steps in the cascade is reduced. Apparently ν_{eff} grows sufficiently fast as E_0 increases to suppress the cascade.

The source terms also play an important role. In (4) the first term is the source at the frequency ω due to the beating of the pump with the turbulent ion fluctuations and the second term the ion fluctuation-induced scattering-in term. The ion density (ion line) power spectrum $\langle |n(\mathbf{k},\omega)|^2\rangle$ in Fig. 2 has, in addition to the familar peaks at $\omega = \pm kc_s$, a feature at $\omega = 0$. We identify this with the ion density fluctuation during collapse which is driven by a ponderomotive force which has a power spectrum centered at $\omega = 0$ and a width $\Delta\omega \lesssim 2\pi/\tau_c$, where τ_c is the caviton lifetime. Such an enhanced $\omega = 0$ feature has been observed at Arecibo[14,15] and is not accounted for in WTT. The peaks at $\omega = \pm kc_s$ are generated by the free-ion sound waves radiated following collapse or by the decay interaction.

The spectral features of the ion line for a given $\mathbf{k}$ are essentially independent of ω_0, i.e., of altitude, unlike the features of the plasma line. The three peaks in the ion line power spectrum produce three peaks in the pump beat-source term in (4), at $\omega = \omega_0 \pm kc_s$ and $\omega = \omega_0$. For *resonant* FLW's where $\omega = \omega_k$, these three peaks occur at the Stokes ($k = k_1$), anti-Stokes ($k = k_a$), and zero-frequency shift, "OTSI" ($k_0 = \omega_0^{1/2}$), modes, respectively. The Stokes or decay line mode k_1 is most strongly excited because its total damping is *reduced* by the parametric decay coupling to the pump in (3) whereas the damping for the anti-Stokes line is *increased.* The OTSI mode *damping* is, to first approximation, uneffected by direct coupling to the pump. The modes excited by this beat-source term at $\omega_{k_0} \simeq \omega_0$ initiate secondary cascades to lower k. Signatures of the beat-source term are particularly clear in the (single realization) power spectra of nonresonant modes *not* in the primary cascade such as $k_x = 9.36$ in Fig. 2 and agree *qualitatively* with the predictions of the ensemble-averaged theory. The cascades originating near k_0 are independent of the primary decay cascade originating from k_1 and contribute to the free-mode component of the modes in the energy spectrum $\langle |\mathbf{E}(\mathbf{k})|^2 \rangle$, which lie between the primary cascade modes.

The mechanism for caviton nucleation appears to depend strongly on ω_0, i.e., on altitude. Evidence for this is obtained by calculating the injection spectrum[3] and by the properties of the decaying turbulence following pump switch off. Near critical density ($\omega_0 \sim 0$) the nucleation is driven directly by the pump,[4] E_0, and we observe that collapse events cease, within a caviton lifetime τ_c, after E_0 is set to zero. In underdense regimes ($\omega_0 > 0$), such as in Fig. 3, after E_0 is turned off, collapse events continue for times long compared to τ_c. During this decay the 1 line decays with a faster rate than the 3 line, etc. The long-wavelength FLW's, which have the longest lifetime, appear to be the driving fields for nucleation. Observations by Fejer, Sulzer, and Djuth,[7] in which the broad spectrum due to caviton collapse at reflection altitude decayed much faster after heater switch off than the cascadelike spectrum at lower altitudes, are consistent with our simulation results. *The observed slow decay of the cascade spectrum and its altitude dependence are not consistent with the caviton correlation description of this spectrum proposed in I.* The free-mode–caviton coupling is formally accounted for by the terms $\nu_{\text{cav}}(\mathbf{k})$ and $S_{\text{cav}}(\mathbf{k})$ in (3) and (4).

The radars, of course, measure only fixed values of **k**. The observed *frequency* cascade power spectra must arise as an integrated effect over some range of altitudes. At most altitudes the primary cascade peaks cannot contribute to the integration for the fixed value of **k**, but the background turbulence can. In the integration this background provides the observed enhanced background on which the sharper cascade structures sit. For stronger driving the 3: and 5: cascade peaks become less distinct and the background becomes stronger. We believe that the combination of these effects in the integrated spectrum may account for the often observed "broad bump" in the Arecibo spectra.[14] Nonresonant excitation of the decay line, the OTSI, and the anti-Stokes line is possible for altitudes away from the matching altitude.

This theory may also explain the transition, with increasing laser power, from a discrete cascade spectrum, in the second-harmonic emission spectrum, to a continuous spectrum as observed in laser-plasma experiments.[16–18]

Further studies of the dependence on parameters, such as E_0, ω_0, m_i/m_e, ν_i, ν_e $(k=0)$, θ, etc., which are needed to make detailed comparison with observations, will be reported elsewhere.

Recently, Hanssen and Mjølhus[19] have reported on 1D simulations of Zakharov's equations. They also observed truncated cascades compared with WTT. They do not compute power spectra or comment on ion-density-fluctuation levels.

We wish to acknowledge helpful conversation with Hector Baldis, Peter Cheung, Frank Djuth, Jules Fejer, Alfred Hanssen, Einar Mjølhus, Mike Sulzer, and Peter Young. This research was supported by the U.S. DOE and by NSF-Air Force Geophysical Laboratory Joint Services Contract No. ATM-9020063.

[1] P. Y. Cheung, T. Tanikawa, J. Santoru, D. F. DuBois, Harvey A. Rose, and David Russell, Phys. Rev. Lett. **62**, 2676 (1989).

[2] D. F. DuBois, Harvey A. Rose, and David Russell, Phys. Rev. Lett. **61**, 2209 (1988).

[3] D. Russell, D. F. DuBois, and H. A. Rose, Phys. Rev. Lett. **60**, 581–584 (1988).

[4] D. F. DuBois, Harvey A. Rose, and David Russell, J. Geophys. Res. **95**, 21 221 (1990). Referred to in text as I. See also Phys. Scr. **T30**, 137 (1990).

[5] F. T. Djuth, C. A. Gonzales, and H. M. Ierkic, J. Geophys. Res. **91**, 12 089 (1986).

[6] F. T. Djuth, M. P. Sulzer, and J. H. Elder, Geophys. Res. Lett. **17**, 1893 (1990).

[7] J. A. Fejer, M. P. Sulzer, and F. T. Djuth, J. Geophys. Res. (to be published).

[8] R. L. Showen and D. M. Kim, J. Geophys. Res. **83**, 623 (1978); A. Y. Wong, G. J. Morales, D. Eggleston, J. Santoru, and R. Behnke, Phys. Rev. Lett. **47**, 1340 (1981).

[9] D. F. DuBois and H. A. Rose, Phys. Rev. A **24**, 1476 (1981).

[10] W. L. Kruer and E. J. Valeo, Phys. Fluids **16**, 675 (1973).

[11] J. A. Fejer and Y. Kuo, Phys. Fluids **16**, 1490–1496 (1973).

[12] F. W. Perkins, C. Oberman, and E. J. Valeo, J. Geophys. Res. **79**, 1478–1496 (1974).

[13] D. F. DuBois and M. V. Goldman, Phys. Rev. Lett. **14**, 544 (1965); Phys. Rev. **164**, 207–222 (1967).

[14] J. A. Fejer, C. A. Gonzales, H. M. Ierkic, M. P. Sulzer, C. A. Tepley, L. M. Duncan, F. T. Djuth, S. Gangulys, and W. E. Gordon, J. Atmos. Terr. Phys. **47**, 1165 (1985).

[15] P. Y. Cheung (private communication).

[16] K. Tanaka, W. Seka, L. M. Goldman, M. C. Richardson, R. W. Short, J. M. Soures, and E. A. Williams, Phys. Fluids **27**, 2187 (1984).

[17] K. Mizuno, P. E. Young, W. Seka, R. Bahr, J. S. de Groot, R. P. Drake, and K. G. Estabrook, Phys. Rev. Lett. **65**, 428 (1990).

[18] H. A. Baldis and P. E. Young, in Proceedings of the Workshop on Chaotic Phenomena in Plasmas, Solids and Fluids, Edmonton, Canada, 16–27 July 1990 (to be published).

[19] A. Hanssen and E. Mjølhus, AGARD Conf. Proc. **485**, 9 (1990).